

# ORMOT: A Dataset and Framework for Omnidirectional Referring Multi-Object Tracking

Sijia Chen<sup>a,1</sup>, Zihan Zhou<sup>a,1</sup>, Yanqiu Yu<sup>a</sup>, En Yu<sup>a</sup>, Wenbing Tao<sup>a,\*</sup>

<sup>a</sup>State Key Laboratory of Multispectral Information Intelligent Processing Technology, School of Artificial Intelligence and Automation, Huazhong University of Science and Technology, Wuhan, 430074, Hubei, China

---

## Abstract

Multi-Object Tracking (MOT) is a fundamental task in computer vision, aiming to track targets across video frames. Existing MOT methods perform well in general visual scenes, but face significant challenges and limitations when extended to visual-language settings. To bridge this gap, the task of Referring Multi-Object Tracking (RMOT) has recently been proposed, which aims to track objects that correspond to language descriptions. However, current RMOT methods are primarily developed on datasets captured by conventional cameras, which suffer from limited field of view. This constraint often causes targets to move out of the frame, leading to fragmented tracking and loss of contextual information. In this work, we propose a novel task, called **Omnidirectional Referring Multi-Object Tracking (ORMOT)**, which extends RMOT to omnidirectional imagery, aiming to overcome the field-of-view (FoV) limitation of conventional datasets and improve the model's ability to understand long-horizon language descriptions. To advance the ORMOT task, we construct **ORSet**, an Omnidirectional Referring Multi-Object Tracking dataset, which contains 27 diverse omnidirectional scenes, 848 language descriptions, and 3,401 annotated objects, providing rich visual, temporal, and language information. Furthermore, we propose **ORTrack**, a Large Vision-Language Model (LVLM)-driven framework tailored for Omnidirectional Referring Multi-Object Tracking. Extensive experiments on the ORSet dataset demonstrate the effectiveness of our ORTrack framework. The dataset and code will be open-sourced at <https://github.com/chen-si-jia/ORMOT>.

*Keywords:* Omnidirectional Cameras, Referring Multi-Object Tracking, ORSet Dataset, ORTrack Framework

---

## 1. Introduction

Multi-Object Tracking (MOT) is a fundamental research topic in computer vision, widely applied in scenarios such as autonomous driving [1] and video surveillance [2]. While existing MOT methods have achieved remarkable success in general visual scenarios, they struggle to handle vision-language scenarios, where the goal is to track objects described by language descriptions. To address this, the task of Referring Multi-Object Tracking (RMOT) [3] has been proposed, aiming to track objects that correspond to specific language descriptions.

However, existing RMOT methods are trained and evaluated on datasets captured by conventional cameras with a limited field of view. As a result, when the camera moves or targets leave the frame, the tracking process becomes fragmented and fails to align with long-horizon language descriptions. As illustrated in Figure 1, given the language description "People who push open the door and then go up the stairs.", conventional RMOT models can only perceive a portion of the scene. When the door area is outside the field of view, the model loses key contextual cues from the "push open the door" action and therefore incorrectly tracks all people going upstairs.

To overcome these limitations of conventional cameras, we extend RMOT to omnidirectional imagery, establishing a new task termed **Omnidirectional Referring Multi-Object Tracking (ORMOT)**. The omnidirectional imagery offers two advantages: (1) it provides continuous spatial coverage, ensuring that all relevant targets remain visible throughout the sequence, and (2)

---

\*Corresponding author

Email addresses: [sijiachen@hust.edu.cn](mailto:sijiachen@hust.edu.cn) (Sijia Chen), [m202473798@hust.edu.cn](mailto:m202473798@hust.edu.cn) (Zihan Zhou), [yanqiuyu6@hust.edu.cn](mailto:yanqiuyu6@hust.edu.cn) (Yanqiu Yu), [yuen@hust.edu.cn](mailto:yuen@hust.edu.cn) (En Yu), [wenbingtao@hust.edu.cn](mailto:wenbingtao@hust.edu.cn) (Wenbing Tao)

<sup>1</sup>Equal contribution

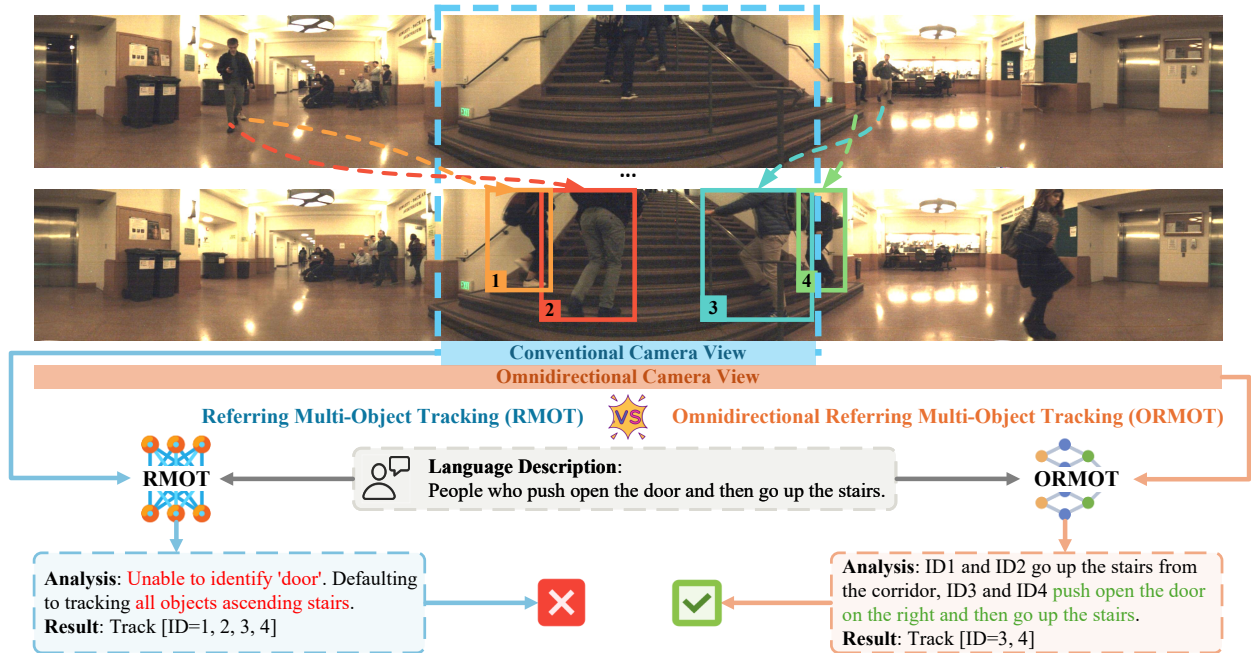


Figure 1: **Comparison between RMOT and ORMOT.** The wide field of view from the omnidirectional camera not only provides spatial advantages but also extends tracking duration by offering "extended temporal context", enabling ORMOT models to correctly understand long-horizon language description and accurately track objects. In contrast, conventional cameras have limited fields of view, making it more difficult for existing common RMOT models to understand long-horizon language description and perform accurate tracking.

it improves language comprehension by capturing a broader spatial context and inter-object relations, which are critical for understanding long-horizon language descriptions (e.g., actions, spatial relations, and group behaviors). As shown in Figure 1, The models of ORMOT can correctly identify the specific objects (ID=3,4) in the action of "push open the door and then go up the stairs" effectively avoiding semantic confusion.

To advance the research on the Omnidirectional Referring Multi-Object Tracking (ORMOT) task, we construct **ORSet**, an Omnidirectional Referring Multi-Object Tracking dataset built upon the JackRabbit Dataset and Benchmark (JRDB) [4]. ORSet contains 848 language descriptions covering omnidirectional-specific characteristics, appearance, and actions, with 3,401 annotated objects and their corresponding bounding boxes and spatiotemporal trajectories across 27 different omnidirectional scenes (17 for training and 10 for testing). This dataset provides a vital platform for researching zero-shot generalization, temporal grounding, and multimodal alignment.

Furthermore, we propose **ORTrack**, a Large Vision-Language Model (LVLM)-driven framework designed for Omnidirectional Referring Multi-Object Tracking. ORTrack leverages the open-vocabulary reasoning and

multimodal understanding of Large Vision-Language Models (LVLMs) [5] to align arbitrary natural language descriptions with 360° visual scenes. Unlike conventional detectors restricted to predefined categories, it supports zero-shot, language-guided detection and tracks objects across frames without category-specific retraining. To ensure robust identity preservation in omnidirectional imagery, ORTrack employs a two-stage cropping-based feature extraction that captures both global contextual cues and fine-grained local details, followed by cross-frame association via feature similarity and Hungarian matching [6]. This design enables flexible and accurate referring multi-object tracking in complex 360° environments.

Finally, we evaluate our ORTrack framework on the ORSet dataset under zero-shot conditions, comparing it with representative open-source RMOT methods. The results show that ORTrack achieves state-of-the-art (SOTA) performance, outperforming other methods in both detection and association metrics. Notably, it demonstrates robust identity preservation, high recall, and strong generalization to unseen objects and complex omnidirectional scenes, highlighting its effectiveness for omnidirectional referring multi-object tracking.

In summary, our main contributions are as follows:

- We propose a novel task, called **Omnidirectional Referring Multi-Object Tracking (ORMOT)**, which extends RMOT to omnidirectional imagery. This setting not only alleviates the field-of-view (FoV) limitation of conventional cameras but also improves the model’s ability to understand long-horizon language descriptions.
- We construct **ORSet**, an Omnidirectional Referring Multi-Object Tracking dataset, which includes 27 different omnidirectional scenes, 848 language descriptions, and 3,401 annotated objects, serving as a comprehensive platform for research on the omnidirectional referring multi-object tracking task.
- We propose **ORTrack**, a Large Vision-Language Model (LVLM)-driven framework designed for Omnidirectional Referring Multi-Object Tracking. Extensive experiments on the ORSet dataset demonstrate that the ORTrack framework achieves **state-of-the-art (SOTA)** performance, validating its effectiveness in complex 360° scenarios, providing a baseline for the ORMOT task.

## 2. Related Work

### 2.1. Multi-Object Tracking

Multi-object tracking (MOT) aims to maintain consistent object identities across video frames. Early methods follow the tracking-by-detection paradigm [7–11], where detections are linked over time using motion and appearance cues. Although simple and effective, these pipelines depend heavily on detector quality and often struggle in crowded or occluded scenes. To improve robustness, joint detection-and-tracking frameworks [12–17] integrate localization and association in an end-to-end manner by learning deep re-identification features, leading to better spatial-temporal consistency. Transformer-based trackers [18–25] further enhance temporal reasoning and global context modeling through self-attention, achieving stronger long-range association and occlusion handling. Recent research trends focus on unified paradigms. MOTIP [25] reformulates MOT as an identity prediction task, directly decoding object IDs without explicit data association.

### 2.2. Referring Multi-Object Tracking

Referring Multi-Object Tracking (RMOT) guides the tracking of multiple objects in videos through language descriptions, enabling more flexible and semantically aware multi-object association. Research in this field

can be broadly categorized into two types. End-to-end methods integrate language grounding and object tracking into a unified optimization framework, thereby enhancing cross-modal reasoning and temporal consistency. For instance, TransRMOT [3] employs a Transformer architecture to jointly model visual and textual information, TempRMOT [26] stabilizes object trajectories via temporal language attention, and ROMOT [27] improves object association in open-set scenarios through enhanced expression understanding. In contrast, two-stage methods first generate object trajectories and then match them with the corresponding language descriptions. iKUN [28] presents an identity-matching mechanism that does not require retraining, while ReferGPT [29] leverages large pre-trained vision-language models to achieve zero-shot referring tracking. CDRMT [30] further enhances multimodal integration through cognitive decoupling. CRMOT [31] extends RMOT to cross-view settings, enabling language-guided identity association across different viewpoints. DRMOT [32] introduces an RGBD referring multi-object tracking dataset and a unified L-RGB-D framework that leverages depth-aware grounding and depth-assisted association to improve trajectory linking and identity preservation under depth-sensitive descriptions and heavy occlusion. RT-RMOT [33] introduces an RGB-Thermal referring multi-object tracking dataset and a unified L-RGB-T framework that exploits thermal cues for robust language-guided trajectory association and identity maintenance under low-light conditions.

### 2.3. Omnidirectional Perception

Omnidirectional perception aims to understand 360° visual data, yet the widely adopted equirectangular projection (ERP) often introduces distortions. To address this issue, the Spherical Vision Transformer [34] partitions the sphere into tangent patches and applies Transformer-based long-range modeling to capture global context; OmniStereo [35] fuses multi-fisheye inputs for real-time depth estimation; and Dense360 [36] provides semantic and geometric annotations to facilitate scene understanding from single omnidirectional images. Progress in this field also benefits from the development of large-scale datasets and generative models: Leader360V [37] offers real-world 360° videos, VideoPanda [38] introduces a diffusion-based framework for omnidirectional video synthesis, Matrix-3D [39] constructs explorable 3D environments from single omnidirectional views, and PanoVid [40] mitigates generation distortions through latitude-aware sampling and rotational denoising. Building upon these advances, omnidirectional multi-object tracking has emerged as a

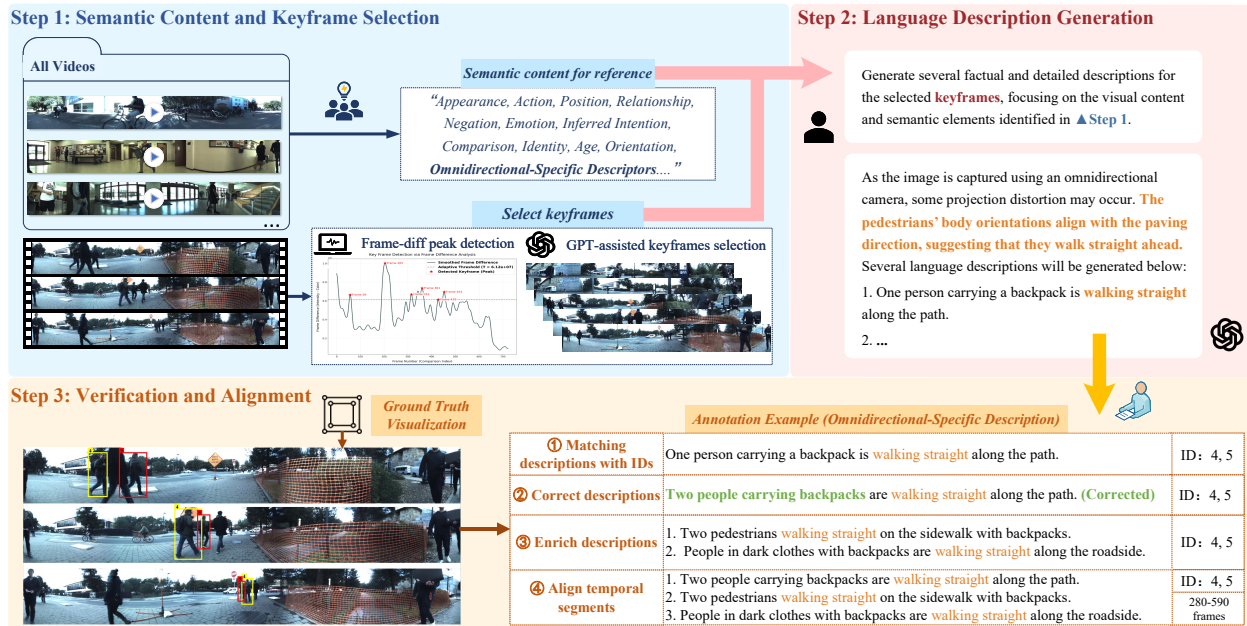


Figure 2: **Overview of the multi-stage language description annotation pipeline.** This pipeline includes three-step: (1) **Step 1** involves selecting the semantic content for reference and identifying representative keyframes through a combination of algorithmic detection and GPT-assisted refinement. (2) **Step 2** leverages a large language model (GPT-4o) to generate diverse and factual descriptions based on the selected keyframes and predefined content. (3) **Step 3** ensures data quality by matching each description to the corresponding person IDs in the visualized ground truth, verifying the accuracy of descriptions, enriching linguistic expressions, and aligning them with temporal segments in the video.

key research direction. MMPAT [41] enhances object detection and trajectory inference by fusing 2D omnidirectional views with 3D point clouds, while OmniTrack [42] integrates Tracklet Management with CircularStatE, effectively combining temporal reasoning and geometric compensation to achieve state-of-the-art performance on omnidirectional tracking benchmarks.

#### 2.4. Large Vision-Language Models

Large Vision-Language Models (LVLMs) have evolved from vision-language alignment to multimodal reasoning. Early efforts such as CLIP [43] established image-text alignment, while recent systems integrate visual encoders directly into large language models. GPT-4 [44], Gemini [45] and Claude extend multimodal understanding through unified perception and reasoning. The latest GPT-5 further enhances long-context reasoning with efficient multimodal fusion. Recent LVLMs emphasize video comprehension and temporal grounding. MiniGPT-5 [46] and InternVL2 [47] improve multi-frame reasoning and scalable multimodal learning. Qwen2.5-VL [5] enhances fine-grained visual grounding, while models such as LongVU [48], FlashVStream [49], Florence2 [50], Emu3 [51], and Pixtral [52] push the boundaries of efficient video-language modeling and instruction tuning.

ChatTracker [53] leverages multimodal large language models to enhance tracking performance.

### 3. Dataset

#### 3.1. Dataset Collection

Our dataset is built upon the JackRabbit Dataset and Benchmark (JRDB) [4]. By employing omnidirectional capture rather than conventional forward-facing views, the JRDB dataset offers a complete and continuous observation of the surrounding environment. This design reduces occlusion and viewpoint bias, providing richer contextual information for scene understanding and tracking research. The original dataset provides essential spatiotemporal annotations for tracking tasks, with each frame labeled with person IDs and bounding boxes. However, it lacks the high-level semantic descriptions necessary for language-guided tasks, limiting its applicability to multimodal research. To address this limitation, we introduce ORSet, a new dataset featuring comprehensive omnidirectional language descriptions that capture both spatial and temporal semantics. This enhancement enables language-driven multimodal research under omnidirectional perception settings.

### 3.2. Dataset Annotation

To ensure high-quality and well-aligned language description annotations, we design a systematic three-stage annotation pipeline, as illustrated in Figure 2.

#### Step 1: Semantic Content and Keyframe Selection.

We systematically review all videos to determine what to describe, including each person’s appearance, movements or postures, spatial relationships with the environment, intentions, emotions, identities, social interactions, and the distinctive trajectories captured by omnidirectional cameras. To locate representative segments, we adopt an algorithmic keyframe selection method based on frame-difference peak detection. Specifically, we compute frame-wise differences to measure visual changes over time and smooth the resulting signal to suppress noise. Local maxima that exceed an adaptive threshold are selected as candidate peaks, representing moments with significant motion or scene variation. Consecutive peaks that are too close are merged to avoid redundancy. To further ensure that the selected moments correspond to semantically meaningful events such as direction changes or occlusions, we perform a GPT-assisted refinement that filters and adjusts these candidates based on textual and visual cues.

**Step 2: Language Description Generation.** We adopt a large language model (LLM) to assist in generating textual trajectory descriptions. Specifically, we employ GPT-4o [44] to produce candidate descriptions based on sampled keyframes and manually summarized semantic references from **Step 1**. A fixed prompt template (as shown in Figure 2, Step 2) is used to ensure consistency in language generation. Specifically, for each trajectory, the LLM generates multiple candidate descriptions focusing on the individuals and their motion patterns within the scene. Subsequently, human annotators match these descriptions with the corresponding ground-truth trajectory IDs visualized in the video. The descriptions are then manually refined, temporally aligned with the trajectory spans, and edited to ensure semantic accuracy and consistency across frames.

**Step 3: Verification and Alignment.** After visualizing the ground-truth annotations, we begin by matching each generated description with its corresponding person ID to establish accurate identity association. Subsequently, we conduct a thorough verification of all descriptions to ensure correctness, followed by refining and enriching their linguistic expressions for clarity and coherence. Finally, each verified description is precisely aligned with its corresponding temporal segment, completing the annotation process.

**Omnidirectional-Specific Descriptors.** Omnidirectional imagery exhibits two prominent characteris-

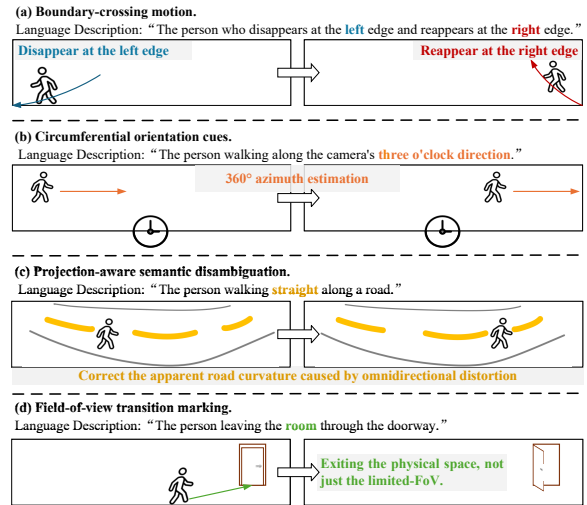


Figure 3: **Visualization of the four omnidirectional-specific descriptors.** (a) Boundary-crossing motion links disappearing and reappearing objects, resolving seam ambiguity. (b) Circumferential orientation cues use a 360° coordinate system for globally consistent direction. (c) Projection-aware semantic disambiguation to understand real motion in scenes. (d) Field-of-view transition marking distinguishes physical exits from view limitations.

tics: (i) full 360° field-of-view coverage, which enables motion and exit behaviors to be described through coordinate- and orientation-aware cues; and (ii) projection-induced distortion and stitching artifacts, which may introduce misleading visual patterns in the scene. Based on these characteristics, we categorize omnidirectional-specific descriptions into four types, as illustrated in Figure 3. In practice, these descriptors are annotated either alone or in combination, reflect overlapping semantics in real scenes.

(a) **Boundary-crossing motion.** When an omnidirectional view is unfolded, seams may cause continuous motion to appear as if an object disappears on one side and reappears on the other. We explicitly describe this phenomenon to help the model recognize it as a single continuous 3D motion (e.g., "A person disappears at the left edge and reappears at the right edge.") rather than two separate targets.

(b) **Circumferential orientation cues.** By leveraging the 360° coordinate system of omnidirectional cameras, we can express directions precisely (e.g., "at the 12 o'clock position"). This observer- or camera-centered anchoring ensures globally consistent and intuitive orientation information, overcoming the ambiguity of relative expressions such as "left" or "right".

(c) **Projection-aware semantic disambiguation.** Due to omnidirectional projection, structurally continuous ele-

Table 1: Statistics of the ORSet dataset.

| Statistic                             | Value      |
|---------------------------------------|------------|
| Video Scenes                          | 27         |
| Total BBoxes                          | 2.9 M      |
| Language Descriptions                 | 848        |
| Omnidirectional-specific Descriptions | 175        |
| Average Frames per Description        | 575.3      |
| Average Description Length            | 8.2 words  |
| Camera State (Static / Moving)        | 13 / 14    |
| Image Size                            | 3760 × 480 |

ments in the real world (e.g., roads or building edges) may appear curved or stretched in the panoramic image. During the annotation process, we leverage environmental geometric cues, such as lane markings and shadow directions, to help annotators infer the true motion direction of targets. These cues are used to guide semantic interpretation during annotation. The original images remain unchanged throughout the process.

(d) Field-of-view transition marking. In omnidirectional scenes, objects may enter or exit the 360° field of view from any direction. We explicitly annotate such events (e.g., "A person leaving the room through the doorway.") to help the model build a coherent understanding of scene dynamics.

### 3.3. Dataset Split

To strike a balance between providing sufficient data for model learning and retaining an adequate number of unseen samples for robust performance evaluation, we split all video sequences in the ORSet dataset into training and test sets at a 6:4 ratio. Language descriptions, person identities, and location information are all tied to the video sequences and are accordingly assigned to the corresponding subsets. This results in a training set containing 17 different omnidirectional scenes and a test set comprising 10 diverse omnidirectional scenes.

### 3.4. Dataset Statistics

The detailed statistics of our ORSet dataset are summarized in Table 1, and the annotation format is illustrated in Listing 1. Other statistical data are as follows:

#### 3.4.1. Word Cloud

As illustrated in Figure 4 (a), the word cloud visualizes the lexical distribution of language descriptions in the dataset. Prominent terms such as "wearing", "edge", "hand", "black", "camera", and "walking" stand out, with words related to appearance (e.g., "black", "shirt",

Listing 1: Annotation format of the ORSet dataset.

```
{
  "scene_id": "bytes-cafe-2019-02-07_0",
  "frame_range": {
    [120, 450],
    [600, 860]
  },
  "annotations": {
    "120": [
      {"id": 3, "bbox": [x1, y1, x2, y2]}
    ],
    "121": [
      {"id": 3, "bbox": [x1, y1, x2, y2]},
      {"id": 8, "bbox": [x1, y1, x2, y2]}
    ],
    ...
  },
  "description": "The person who orders food."
}
```

"shoes", "clothes") and action (e.g., "walking", "carrying", "holding") appearing frequently. These two categories represent common features used in daily life to describe people, making the annotations highly intuitive and aligned with human cognitive habits. Notably, the high frequency of "edge" results from the inclusion of Omnidirectional-Specific Descriptors in our dataset, which capture the unique characteristics of omnidirectional imagery and highlight the dataset's novelty and distinction from general vision–language datasets.

#### 3.4.2. Distribution of Language Description Types

The dataset contains diverse description types, which we categorize into three main groups: Appearance, Action, and Omnidirectional-specific descriptors, as depicted in Figure 4 (b). The three main categories are: Appearance (332), Action (182), and Omnidirectional-specific descriptors (46), where the numbers represent the count of descriptions belonging solely to these types. Additionally, descriptions that combine these three categories are also counted, as indicated by the "+" nodes in the figure. Each main category is associated with multiple related sub-types; for example, Omnidirectional-specific descriptors include unique aspects like Edge, relative perspective, FoV, and distortion correction. The "Shared and Cross-listed Categories" node, within the "Others" branch, indicates that many sub-categories (e.g., emotion) are not confined to a single main category and can also form descriptions independently. This pattern aligns with real-world commands, which typically integrate multiple attributes rather than relying on a single feature, thereby highlighting the dataset's potential to support research on complex language–vision alignment.

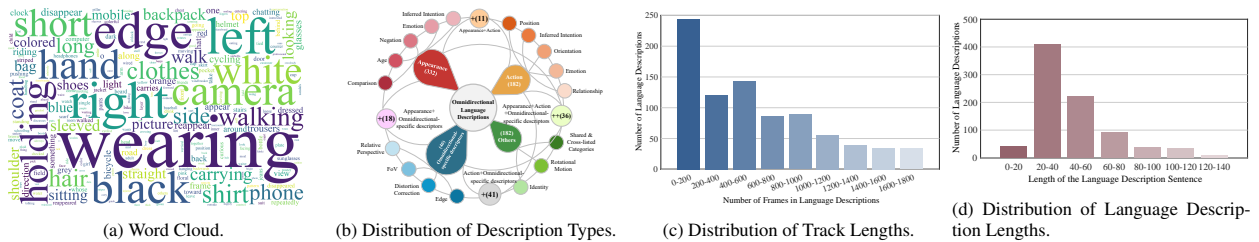


Figure 4: **Overview of the ORSet dataset statistics.** (a) **Word Cloud:** Frequent terms primarily cover appearance (e.g., "wearing", "black"), actions (e.g., "walking"), and omnidirectional-specific cues (e.g., "edge"). The vocabulary's diversity indicates that the annotations are rich and cover multifaceted information, while terms like "edge" reflect the unique properties of omnidirectional imagery. (b) **Distribution of Language Description Types:** Descriptions are mainly categorized into appearance, action, and omnidirectional-specific descriptors. Most descriptions are compositional, blending multiple attributes. (c) **Distribution of Language Description Lengths:** The majority of descriptions are concentrated in the 20-80 character range, suggesting the annotation language description is concise. (d) **Distribution of Track Lengths:** The dataset provides balanced coverage across short- and long-term tracks, supporting comprehensive temporal reasoning for long-horizon language descriptions.

### 3.4.3. Distribution of Language Description Lengths

We analyze the length of language descriptions in terms of the number of characters, as shown in Figure 4 (c). The results reveal that most descriptions fall within a moderate range, primarily between 20 and 80 characters, while a smaller portion extends beyond 100 characters. This distribution suggests that the dataset contains both concise and relatively detailed expressions, reflecting natural variability in human descriptions. Importantly, the dominance of short-to-medium sentences indicates that the annotations are consistent with everyday spoken language habits, where expressions tend to be succinct and focused on key observable events. Such language characteristics make the dataset well-suited for studying natural and coherent language generation aligned with visual content.

### 3.4.4. Distribution of Track Lengths

To examine the temporal span of the language descriptions in the ORSet dataset, we calculate the number of frames covered by each description, which reflects the trajectory length of the described event. As shown in Figure 4 (d), most descriptions correspond to short sequences within 0–200 frames, followed by a gradual decrease as the frame range increases. Medium-length descriptions (200–1000 frames) maintain a moderate presence, while long sequences exceeding 1000 frames are relatively rare. This long-tailed distribution indicates that the dataset predominantly contains concise, observable actions, yet still includes a sufficient number of long-duration cases, which is particularly beneficial for the Omnidirectional Referring Multi-Object Tracking setting. Such a composition provides a balanced coverage of both short-term and long-term temporal contexts, supporting fine-grained temporal grounding and robust vision-language alignment.

## 4. Methodology

### 4.1. Overview

We propose ORTrack, an Omnidirectional Referring Multi-Object Tracking framework that leverages the open-vocabulary reasoning capability of large vision-language models (LVLMs) to detect and associate multiple referred objects in omnidirectional scenes. Unlike conventional detectors trained on fixed taxonomies, our method allows arbitrary language queries to guide multi-object tracking in complex and omnidirectional environments. Given a sequence of omnidirectional frames  $\{I_t\}_{t=1}^T$  and a language description  $L$ , ORTrack produces a set of trajectories  $\mathcal{T} = \{\tau_k\}_{k=1}^K$ , where each  $\tau_k = \{b_t^k\}_{t=t_s}^{t_e}$  represents a continuous tracklet corresponding to a language-referred target. The pipeline of our ORTrack framework is shown in Figure 5.

### 4.2. Language-guided Detection via LVLM

Omnidirectional environments cover  $360^\circ$  fields of view, often containing multiple entities with varying appearances and scales. Conventional detectors suffer from limited predefined classes and lack flexibility to respond to language descriptions. To address this, ORTrack employs an LVLM-based detection mechanism that integrates visual grounding and semantic understanding in a unified reasoning process. Given a frame  $I_t$  and a text instruction  $L$ , the LVLM (e.g., Qwen2.5-VL [5], InternVL3.5 [54]) internally performs: (1). Visual encoding:  $\psi_v(I_t)$  to obtain visual tokens. (2). Language encoding:  $\psi_l(L)$  to represent the instruction. (3). Multi-modal cross-attention reasoning to align language with visual regions. (4). Bounding box prediction for the referred targets. Formally:

$$\{b_t^i\}_{i=1}^{N_t} = \text{LVLM}(I_t, L) = \text{Align}(\psi_v(I_t), \psi_l(L)) \quad (1)$$

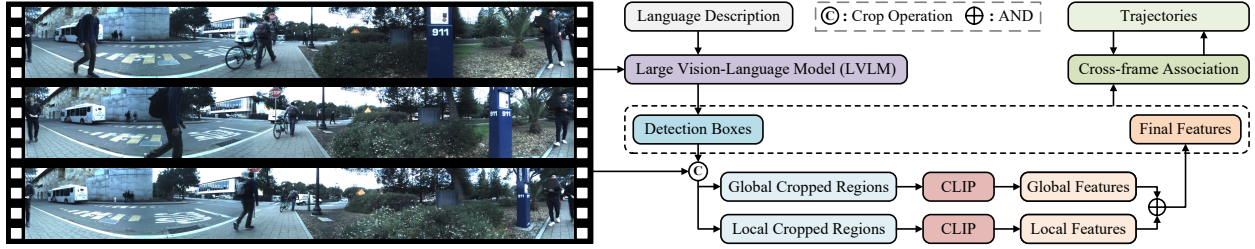


Figure 5: **Pipeline of ORTrack.** It comprises three components: (1) **Language-guided detection via LVL:** Using a Large Vision-Language Model (LVL) as an open-vocabulary detector to output bounding boxes conditioned on the language description. (2) **Two-stage cropping-based feature extraction:** Hierarchical region extraction and feature encoding to obtain discriminative features. (3) **Cross-frame association:** Linking detected boxes via cosine similarity and Hungarian matching to maintain consistent object identities.

where  $b_t^i = (x_t^i, y_t^i, w_t^i, h_t^i)$  represents the bounding box of the  $i$ -th referred object.

#### 4.3. Two-stage Cropping-based Feature Extraction

Following LVL-based detection, ORTrack performs two-stage cropping-based inference to obtain robust object features, effectively balancing global contextual cues and local discriminative details. Given that omnidirectional images are represented in an equirectangular projection, where objects may extend from the leftmost to the rightmost boundaries, IoU-based matching becomes unreliable. Therefore, ORTrack employs a feature-based association strategy to maintain consistent identities across the omnidirectional view.

**Stage 1: Global Contextual Cropping.** Omnidirectional frames often suffer from wide-angle compression, which can destabilize local features. To mitigate this effect, each detected box is expanded by a margin ratio  $\alpha$  to incorporate surrounding contextual information:

$$I_t^{i, \text{global}} = \text{Crop}(I_t, \alpha b_t^i) \quad (2)$$

where  $I_t^{i, \text{global}}$  represents the global cropped region of the  $i$ -th referred object. The "Crop( $\cdot$ )" represents the cropping operation.  $I_t$  represents the frame.  $\alpha$  represents the margin ratio.

**Stage 2: Fine-grained Target Cropping.** The second-stage crop extracts the exact target region  $I_t^{i, \text{local}}$ , defined by the detected bounding box  $b_t^i$ .

$$I_t^{i, \text{local}} = \text{Crop}(I_t, b_t^i) \quad (3)$$

where  $I_t^{i, \text{local}}$  represents the local cropped region of the  $i$ -th referred object. The "Crop( $\cdot$ )" denotes the cropping operation.  $I_t$  denotes the frame.

Both global and local regions are processed by a frozen CLIP [43] visual encoder to generate features:

$$\mathbf{f}_{t, \text{global}}^i = \phi_g(I_t^{i, \text{global}}) \quad (4)$$

$$\mathbf{f}_{t, \text{local}}^i = \phi_l(I_t^{i, \text{local}}) \quad (5)$$

where  $\mathbf{f}_{t, \text{global}}^i$  represents the global feature of the  $i$ -th referred object.  $\mathbf{f}_{t, \text{local}}^i$  represents the local feature of the  $i$ -th referred object.  $\phi$  denotes the CLIP visual encoder.

The final object feature is computed as follows:

$$\mathbf{f}_t^i = \mathbf{f}_{t, \text{local}}^i + \lambda \mathbf{f}_{t, \text{global}}^i \quad (6)$$

where  $\mathbf{f}_t^i$  represents the feature of the  $i$ -th referred object.  $\lambda$  represents the feature fusion weight of  $\mathbf{f}_{t, \text{global}}^i$ .

#### 4.4. Cross-frame Association

To maintain identity consistency, ORTrack adopts cosine-similarity-based matching followed by Hungarian algorithm. Specifically, given two consecutive frames  $t$  and  $t+1$ , we compute the pairwise cosine similarity between all detected objects to construct a similarity matrix. Formally,

$$S_{ij} = \frac{\mathbf{f}_t^i \cdot \mathbf{f}_{t+1}^j}{\|\mathbf{f}_t^i\| \|\mathbf{f}_{t+1}^j\|} \quad (7)$$

where  $\mathbf{f}_t^i$  and  $\mathbf{f}_{t+1}^j$  denote the visual embeddings of the  $i$ -th and  $j$ -th objects in frames  $t$  and  $t+1$ , respectively.

The corresponding cost matrix is defined as  $C_{ij} = 1 - S_{ij}$ , which is used to find the optimal one-to-one assignment via Hungarian algorithm [6]:

$$\min_X \sum_{i,j} C_{ij} X_{ij}, \quad \text{s.t. } X_{ij} \in \{0, 1\}. \quad (8)$$

where  $X_{ij} = 1$  indicates that detection  $j$  in frame  $t+1$  is assigned to track  $i$  in frame  $t$ .

This process ensures consistent identity propagation across frames while minimizing the overall association cost. Unmatched detections initiate new tracklets, while tracks without matches for  $\tau_{\text{max}}$  frames are terminated.

Table 2: **Performance of different methods** on the test set of the ORSet dataset under zero-shot conditions.  $\uparrow$  indicates that higher score is better. The best results are marked in **bold**.

| Method                | Published  | HOTA $\uparrow$ | DetA $\uparrow$ | AssA $\uparrow$ | DetRe $\uparrow$ | DetPr $\uparrow$ | AssRe $\uparrow$ | AssPr $\uparrow$ | LocA $\uparrow$ |
|-----------------------|------------|-----------------|-----------------|-----------------|------------------|------------------|------------------|------------------|-----------------|
| TransRMOT [3]         | CVPR 2023  | 2.41            | 1.40            | 4.24            | 1.56             | 12.10            | 4.29             | 79.29            | 75.05           |
| TempRMOT [26]         | ArXiv 2024 | 2.00            | 0.45            | 9.01            | 0.47             | 11.01            | 9.44             | <b>80.93</b>     | 78.88           |
| <b>ORTrack (Ours)</b> | -          | <b>9.97</b>     | <b>6.37</b>     | <b>16.15</b>    | <b>9.20</b>      | <b>16.69</b>     | <b>17.35</b>     | 61.80            | <b>79.68</b>    |

Table 3: **Ablation study** of our ORTrack framework on the test set of the ORSet dataset under zero-shot conditions. The **number** in the first column indicates the row number.  $\uparrow$  indicates that higher score is better. The best results are marked in **bold**.

| Large Vision-Language Models (LVLMs) |      |                 | Metrics         |                 |                  |                  |                  |                  |                 |  |
|--------------------------------------|------|-----------------|-----------------|-----------------|------------------|------------------|------------------|------------------|-----------------|--|
| Name                                 | Size | HOTA $\uparrow$ | DetA $\uparrow$ | AssA $\uparrow$ | DetRe $\uparrow$ | DetPr $\uparrow$ | AssRe $\uparrow$ | AssPr $\uparrow$ | LocA $\uparrow$ |  |
| <b>1</b> DeepSeek-VL [55]            | 7B   | 0.12            | 0.06            | 0.29            | 0.06             | 2.83             | 0.30             | 17.89            | 66.66           |  |
| <b>2</b> LLaVA-NEXT [56]             | 8B   | 1.76            | 1.11            | 3.12            | 1.55             | 3.35             | 3.80             | 16.22            | 57.57           |  |
| <b>3</b> InternVL3.5 [54]            | 8B   | 0.55            | 0.49            | 0.72            | 0.52             | 6.93             | 0.74             | 39.48            | 61.56           |  |
| <b>4</b> Qwen2.5-VL [5]              | 7B   | <b>9.97</b>     | <b>6.37</b>     | <b>16.15</b>    | <b>9.20</b>      | <b>16.69</b>     | <b>17.35</b>     | <b>61.80</b>     | <b>79.68</b>    |  |
| <b>5</b> Qwen2.5-VL [5]              | 3B   | 3.33            | 2.13            | 5.84            | 2.72             | 8.54             | 6.08             | 52.44            | 71.34           |  |

## 5. Experiments

### 5.1. Metrics

We follow the standard evaluation metrics [3] to evaluate our method. Specifically, the following metrics are employed: Higher Order Tracking Accuracy (HOTA), Detection Accuracy (DetA), Association Accuracy (AssA), Detection Recall (DetRe), Precision (DetPr), Association Recall (AssRe), Precision (AssPr), and Localization Accuracy (LocA), which jointly and comprehensively assess the detection accuracy, association consistency, and localization precision of the overall tracking performance.

### 5.2. Implementation Details

Our ORTrack framework is built upon large vision-language models (LVLMs) and CLIP. Specifically, we adopt Qwen2.5-VL-7B [5] as the large vision-language model (LVLM) backbone and CLIP-ViT-B-32 [43] as the CLIP encoder. The margin ratio  $\alpha$  in Equation (2) is set to 1.2, and the feature fusion weight  $\lambda$  in Equation (6) is set to 0.5. All experiments are conducted on a single NVIDIA RTX A6000 GPU.

To ensure a fair evaluation of different large vision-language models (LVLMs) within the ORTrack framework, we unify the prompt construction strategy across all models while allowing minor adaptations to accommodate their respective instruction formats. Given a language description (e.g., "The person carrying a bag pushed open the door and walked out of the field of view."), each LVLM is asked to detect all targets that

match the language description. For DeepSeek-VL-7B [55], LLaVA-NEXT-8B [56], and InternVL3.5-8B [54], we employ a structured detection-oriented prompt that asks the model to "Please detect all  $\{description\}$  in the image and output their coordinates in the  $[x1, y1, x2, y2]$  format.". For the Qwen2.5-VL series (7B and 3B) [5], whose instruction style emphasizes explicit labeling, the prompts ask the model to "Please detect and label all  $\{description\}$  in the following image and mark their positions.". This unified yet model-aware prompt design ensures that each LVLM performs the referring detection, enabling consistent cross-model comparison and reliable integration into the ORTrack framework.

### 5.3. Quantitative Results

We conduct a comparative evaluation of our ORTrack framework against existing methods on the ORSet dataset under zero-shot conditions. It is worth noting that only open-source RMOT methods are included for fair comparison. As shown in Table 2, the proposed ORTrack consistently outperforms prior works across most evaluation metrics, achieving the best overall performance. In particular, ORTrack attains a substantial improvement in HOTA (9.97 vs. 2.41/2.00), DetA (6.37 vs. 1.40/0.45), and AssA (16.15 vs. 4.24/9.01), indicating enhanced detection robustness and association stability. Moreover, its balanced gains in both DetPr/AssPr and DetRe/AssRe demonstrate strong identity preservation and recall capability, even without fine-tuning on the dataset. These results highlight the remarkable zero-

Table 4: **Efficiency and performance of different feature encoder.**  $\uparrow$  indicates that higher score is better.  $\downarrow$  indicates that lower score is better. The best results are marked in **bold**.

| Method         | Feature      |             | Efficiency     |                               | Metrics         |                 |                 |                  |                  |                  |                  |                 |
|----------------|--------------|-------------|----------------|-------------------------------|-----------------|-----------------|-----------------|------------------|------------------|------------------|------------------|-----------------|
|                | Encoder      | Dims        | FPS $\uparrow$ | FLOPs $\downarrow$            | HOTA $\uparrow$ | DetA $\uparrow$ | AssA $\uparrow$ | DetRe $\uparrow$ | DetPr $\uparrow$ | AssRe $\uparrow$ | AssPr $\uparrow$ | LocA $\uparrow$ |
| w/o CLIP       | <b>LVL</b> M | <b>3584</b> | 0.399          | <b>4.193</b> $\times 10^{13}$ | <b>10.05</b>    | <b>6.37</b>     | <b>16.42</b>    | <b>9.20</b>      | 16.68            | <b>17.65</b>     | 61.74            | <b>79.68</b>    |
| ORTrack (Ours) | <b>CLIP</b>  | <b>512</b>  | <b>0.446</b>   | 4.194 $\times 10^{13}$        | 9.97            | <b>6.37</b>     | 16.15           | <b>9.20</b>      | <b>16.69</b>     | 17.35            | <b>61.80</b>     | <b>79.68</b>    |

Table 5: **Performance of different association strategies on the ORSet dataset.**  $\uparrow$  indicates that higher score is better. The best results are marked in **bold**.

| Method         | HOTA $\uparrow$ | DetA $\uparrow$ | AssA $\uparrow$ | DetRe $\uparrow$ | DetPr $\uparrow$ | AssRe $\uparrow$ | AssPr $\uparrow$ | LocA $\uparrow$ |
|----------------|-----------------|-----------------|-----------------|------------------|------------------|------------------|------------------|-----------------|
| LVL            | 5.05            | 2.56            | 10.19           | 2.83             | <b>20.76</b>     | 10.66            | <b>73.04</b>     | <b>80.70</b>    |
| ORTrack (Ours) | <b>9.97</b>     | <b>6.37</b>     | <b>16.15</b>    | <b>9.20</b>      | 16.69            | <b>17.35</b>     | 61.80            | 79.68           |

shot generalization capacity and powerful tracking performance of our ORTrack framework.

#### 5.4. Ablation Study

To assess the effectiveness of the proposed ORTrack framework, we conduct some ablation experiments on the test set of the ORSet dataset.

#### 5.5. Analysis of Large Vision-Language Models

To investigate the effect of different large vision-language models (LVL

M)s on the ORTrack framework, we evaluate several LVLM)s of comparable scale to Qwen2.5-VL on the ORSet dataset. As shown in Table 3, under zero-shot conditions, ORTrack equipped with Qwen2.5-VL-7B (row 4) achieves the best overall performance across all evaluation metrics, surpassing other LVLM)s such as DeepSeek-VL (row 1), LLaVA-NEXT (row 2), and InternVL3.5 (row 3). Moreover, compared to its smaller counterpart Qwen2.5-VL-3B (row 5), the 7B model exhibits a substantial performance gain, demonstrating that a larger model size with stronger reasoning and visual-language alignment capabilities leads to more accurate and robust language-guided tracking. These results collectively confirm that the selection and capacity of the LVLM play a decisive role in determining the zero-shot generalization and overall effectiveness of the ORTrack framework.

#### 5.6. Analysis of CLIP vs LVLM for Feature Encoder

As shown in Table 4, choosing between CLIP [43] and LVL

M as a feature encoder involves a trade-off between accuracy and computational efficiency. LVLM-based feature encoder achieves slightly higher accu-

racy due to its higher-dimensional feature representations, but this increased dimensionality leads to significant computational overhead, especially during similarity computations. In contrast, CLIP provides a more computationally efficient solution. Although it offers slightly lower accuracy compared to LVL

M, its lower-dimensional feature representations allow for faster processing, resulting in higher FPS and better real-time performance, achieving higher overall efficiency.

#### 5.7. Analysis of Different Association Strategies

As shown in Table 5, we conduct an ablation study to compare ORTrack with LVL

M + OC-SORT, where both methods use LVLM as the object detector, but ORTrack employs a different association strategy than OC-SORT [10]. The results reveal that ORTrack significantly outperforms LVLM + OC-SORT across all metrics. Specifically, ORTrack achieves a substantial improvement in HOTA (9.97 vs. 5.05) and Assignment Accuracy (16.15 vs. 10.19), indicating that ORTrack’s association strategy is more effective in matching objects across frames. Furthermore, ORTrack exhibits higher Detection Accuracy (6.37 vs. 2.56) and Detection Recall (9.20 vs. 2.83), demonstrating that its approach to object tracking leads to more accurate and consistent detections. Although Localization Accuracy is similar between the two methods (79.68 vs. 80.70), ORTrack outperforms OC-SORT in Assignment Recall (17.35 vs. 10.66), highlighting the superior precision of ORTrack’s association strategy. Overall, this ablation study confirms that ORTrack’s association approach provides notable improvements in tracking performance, even when using the same detector as OC-SORT.

**Language Description:** The person skateboarding along a straight road.

**Result:** Track [ID=3]



**Language Description:** The person wearing grayish-white trousers.

**Result:** Track [ID=1, 2]



**Language Description:** Language Description: The person entering the field of vision.

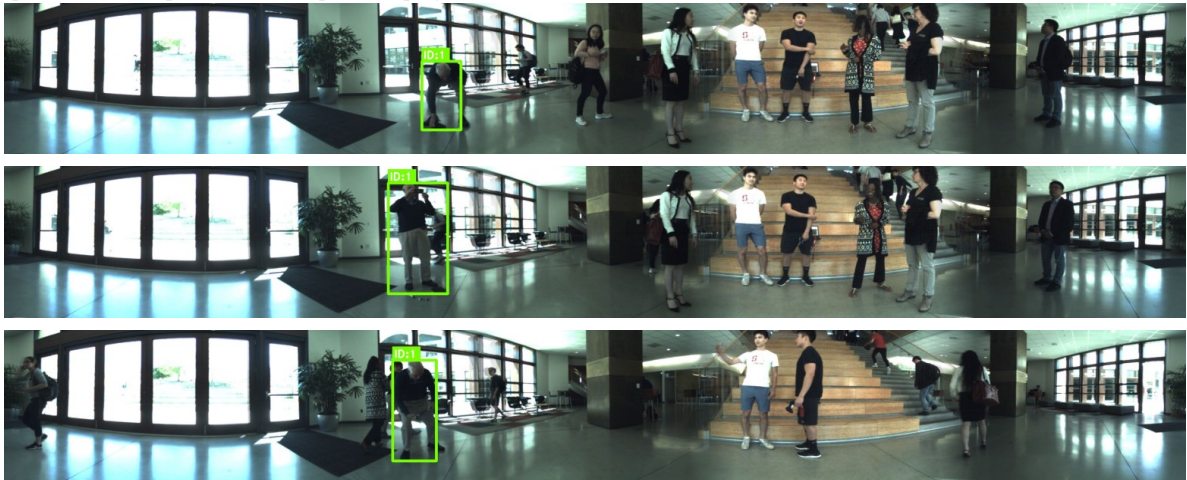
**Result:** Track [ID=12]



Figure 6: **Qualitative results (Part 1)** of our ORTrack framework on the test set of the ORSet dataset under zero-shot conditions.

**Language Description:** The person who puts the thing in their hand on the ground, takes a photo with their phone, and then picks it up again.

**Result:** Track [ID=1]



**Language Description:** People riding bicycles.

**Result:** Track [ID=2, 10]



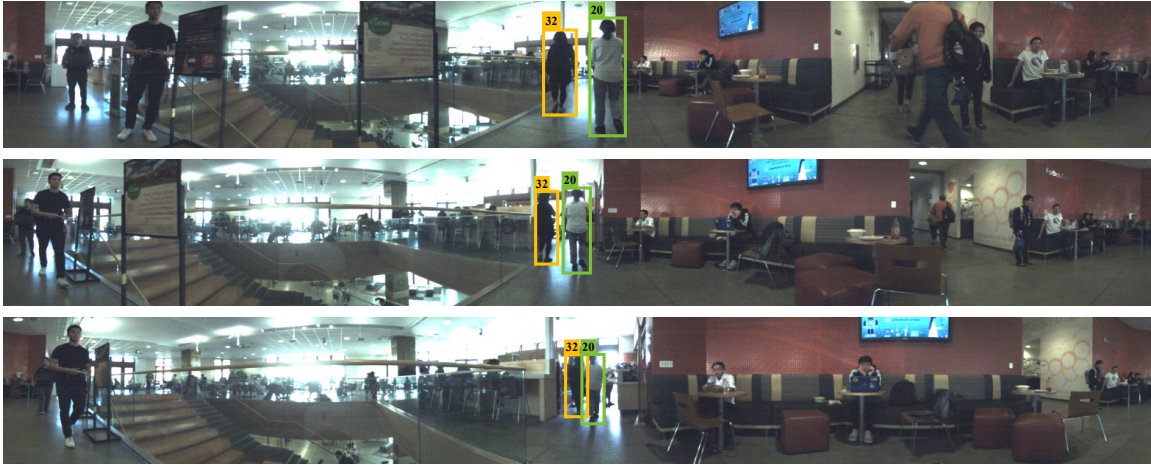
**Language Description:** The person who is happy and looking forward to it, waiting for others to ask. **Result:** Track [ID=1]



Figure 7: **Qualitative results (Part 2)** of our ORTrack framework on the test set of the ORSet dataset under zero-shot conditions.

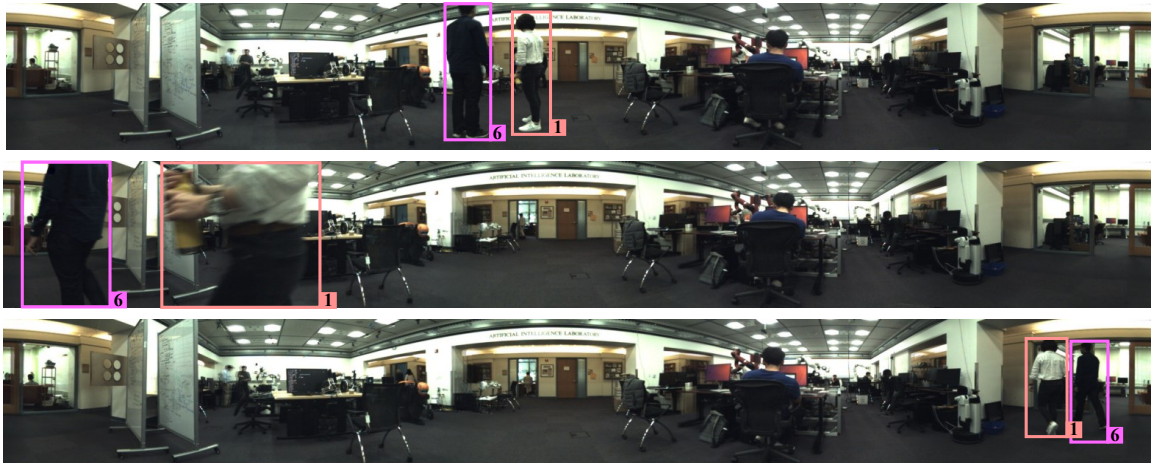
**Language Description:** The person walking forward along the 12 o'clock direction of the camera.

**Ground Truth:** Track [ID=20, 32]



**Language Description:** The person who disappears from the left edge and reappears from the right edge.

**Ground Truth:** Track [ID=1, 6]



**Language Description:** The person who leaves the field of view.

**Ground Truth:** Track [ID=14, 20]



Figure 8: **Representative examples (Part 1)** of language descriptions and ground truth in the ORSet dataset, featuring omnidirectional-specific descriptors.

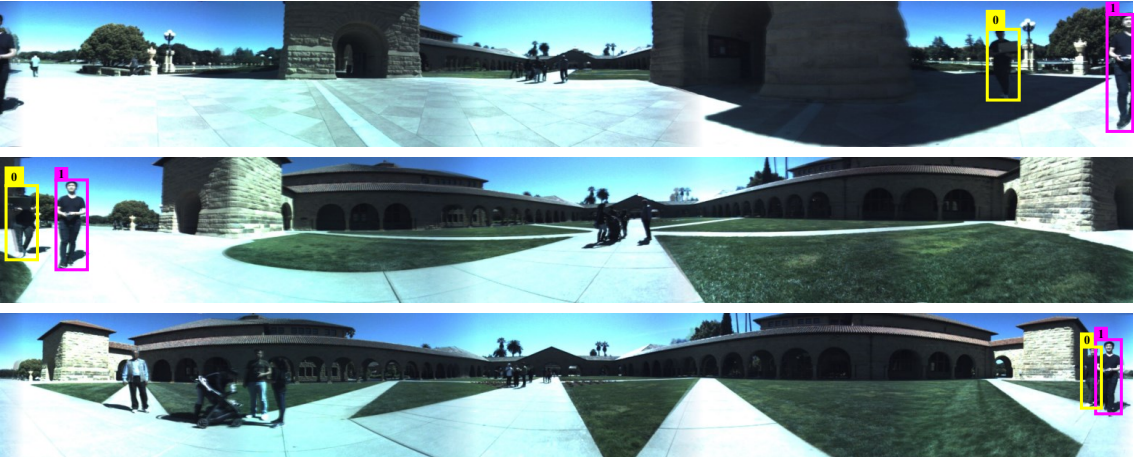
**Language Description:** The person dressed in black, holding a cup in his hand, walked straight along the bushes together.

**Ground Truth:** Track [ID=16, 17]



**Language Description:** Because the camera moves the people who repeatedly appear on the left and right edges.

**Ground Truth:** Track [ID=0, 1]



**Language Description:** The waiter in a black apron walks from the right side of the picture to the left in front of the camera.

**Ground Truth:** Track [ID=39]

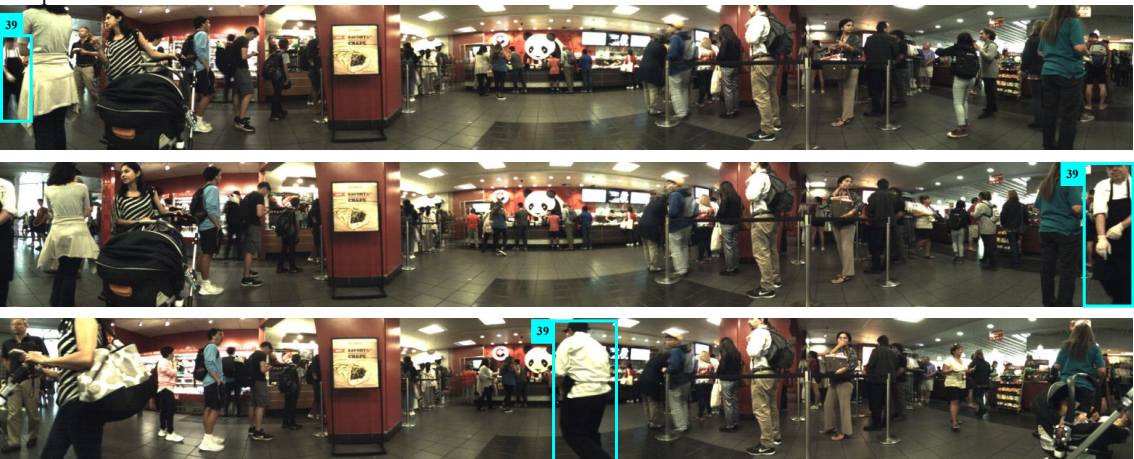


Figure 9: **Representative examples (Part 2)** of language descriptions and ground truth in the ORSet dataset, featuring omnidirectional-specific descriptors.

### 5.8. Qualitative Results of the ORTrack Framework

To further validate the effectiveness of the proposed ORTrack framework, we visualize more results of our ORTrack framework on the test set of the ORSet dataset under zero-shot conditions. Qualitative results are shown in Figure 6 and Figure 7. We find that our ORTrack framework shows zero-shot capability.

For example, in the first example in Figure 6, the road in the image is distorted from straight to curved due to omnidirectional projection, but according to the description "The person skateboarding along a straight road." the target can still be tracked correctly. Moreover, in the last example of Figure 7, for the language description "The person who is happy and looking forward to it, waiting for others to ask.", this is a highly difficult emotion inference task. Although emotion is a subtle and subjective state, the model accurately tracks the target exhibiting the corresponding facial expression or body language.

In summary, ORTrack demonstrates the ability to associate language descriptions with corresponding targets and maintain trajectory tracking under omnidirectional settings.

### 5.9. Language Descriptions and Ground Truth in the ORSet dataset

The ORSet dataset contains a large number of language descriptions that are specific to omnidirectional scenes, reflecting the distinctive properties of 360° visual perception. These descriptions often incorporate inference cues that only arise in omnidirectional environments, such as boundary-crossing behaviors, long-horizon motion paths, and viewpoint-dependent appearance changes.

Figure 8 and Figure 9 show several omnidirectional-specific challenges. For example, in the second case of Figure 8, the language description "The person who disappears from the left edge and reappears from the right edge." explicitly captures the boundary-crossing motion inherent to 360° videos, where a target seamlessly transitions across opposite edges of the equirectangular frame. The last example in Figure 9, with the description "The moving waiter wearing a black apron." demonstrates a challenging long-horizon tracking scenario. The omnidirectional camera captures the target's full extended trajectory (Track ID 39). This case requires the model to overcome two hurdles: maintaining identity continuity despite pose and orientation shifts, and using role-based inference to correctly identify the target's professional role.

### (a) Case1: Detection Failure. (False detections and missed detections)



### (b) Case2: Association Failure. (Target identity switches)

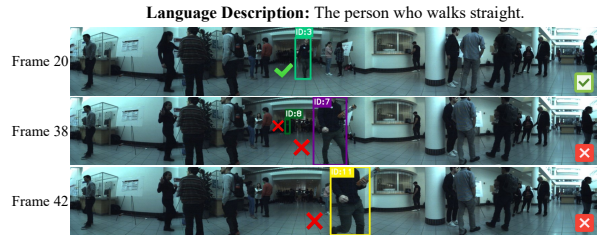


Figure 10: Representative Failure Cases of ORMOT.

Overall, The ORSet dataset contains numerous descriptions that arise from omnidirectional viewing conditions, verifying the dataset's richness, realism, and its unique alignment with 360° scene understanding.

### 5.10. Failure Case Analysis

Representative failure cases are presented in Figure 10 to illustrate the practical challenges of ORMOT under real-world conditions.

In Case 1 (Detection Failure), shown in part (a), the system struggles with false detections and missed detections, which are common issues in omnidirectional video tracking. For instance, in Frame 60, the system incorrectly assigns an ID to a false detection, while in Frame 80, a person carrying a backpack is missed entirely. These issues are exacerbated by the distortion inherent to omnidirectional projections, where the target can be distorted due to changes in the field-of-view (FoV), leading to inaccurate tracking.

In Case 2 (Association Failure), depicted in part (b), the challenge shifts to target identity switches. As shown in the sequence from Frame 20 to Frame 42, the system incorrectly assigns multiple IDs to the same person, especially when a person is moving in close proximity, leading to identity switches. This issue is aggravated by close-range motion, where rapid scale changes and feature drift make it difficult for the model to maintain accurate identity tracking across frames. Such identity switches are critical problems for long-term tracking in dynamic environments, where maintaining consistent associations is crucial.

This trend of detection and association challenges is also reflected in Table 5, where Detection Accuracy (DetA) is generally lower than Assignment Accuracy (AssA) across evaluated methods. The disparity between these metrics highlights the difficulty of achieving both accurate detections and stable associations, particularly in complex and rapidly changing omnidirectional environments.

## 6. Conclusion and Future Work

In this work, we propose a novel task, called **Omnidirectional Referring Multi-Object Tracking (ORMOT)**, which extends RMOT to omnidirectional imagery. This setting not only alleviates the field-of-view (FoV) limitation of conventional cameras but also improves the model’s ability to understand long-horizon language descriptions. To advance the research on the ORMOT task, we construct **ORSet**, an Omnidirectional Referring Multi-Object Tracking dataset, including 27 different omnidirectional scenes, 848 language descriptions, and 3,401 annotated objects. Furthermore, we propose **ORTrack**, a Large Vision-Language Model-driven framework tailored for the ORMOT task. We evaluate the ORTrack framework on the ORSet dataset, which achieves **state-of-the-art (SOTA)** performance, providing a baseline for the ORMOT task.

Future work should focus on two main aspects: first, improving robust detection under omnidirectional distortion; and second, enhancing stable association under severe geometric distortions, such as those caused by target motion and scale variation.

## Acknowledgements

This work was supported by the National Natural Science Foundation of China (Grant 62576144).

## References

- [1] W. Meng, S. Duan, S. Ma, B. Hu, Motion-perception multi-object tracking (mpmot): Enhancing multi-object tracking performance via motion-aware data association and trajectory connection, *Journal of Imaging* 11 (5) (2025) 144.
- [2] Z. Guan, Z. Wang, G. Zhang, L. Li, M. Zhang, Z. Shi, N. Jiang, Multi-object tracking review: retrospective and emerging trend, *Artificial Intelligence Review* 58 (8) (2025) 235.
- [3] D. Wu, W. Han, T. Wang, X. Dong, X. Zhang, J. Shen, Referring multi-object tracking, in: *Proceedings of the IEEE/CVF conference on computer vision and pattern recognition*, 2023, pp. 14633–14642.
- [4] R. Martín-Martín, H. Rezatofighi, A. Sheno, M. Patel, J. Gwak, N. Dass, A. Federman, P. Goebel, S. Savarese, Jrdb: A dataset and benchmark for visual perception for navigation in human environments, *arXiv preprint arXiv:1910.11792* (2019).
- [5] S. Bai, K. Chen, X. Liu, J. Wang, W. Ge, S. Song, K. Dang, P. Wang, S. Wang, J. Tang, et al., Qwen2. 5-vl technical report, *arXiv preprint arXiv:2502.13923* (2025).
- [6] H. W. Kuhn, The hungarian method for the assignment problem, *Naval research logistics quarterly* 2 (1-2) (1955) 83–97.
- [7] A. Bewley, Z. Ge, L. Ott, F. Ramos, B. Upcroft, Simple online and realtime tracking, in: *2016 IEEE international conference on image processing (ICIP)*, IEEE, 2016, pp. 3464–3468.
- [8] N. Wojke, A. Bewley, D. Paulus, Simple online and realtime tracking with a deep association metric, in: *2017 IEEE international conference on image processing (ICIP)*, IEEE, 2017, pp. 3645–3649.
- [9] Y. Zhang, P. Sun, Y. Jiang, D. Yu, F. Weng, Z. Yuan, P. Luo, W. Liu, X. Wang, Bytetrack: Multi-object tracking by associating every detection box, in: *European Conference on Computer Vision*, Springer, 2022, pp. 1–21.
- [10] J. Cao, J. Pang, X. Weng, R. Khrodar, K. Kitani, Observation-centric sort: Rethinking sort for robust multi-object tracking, in: *Proceedings of the IEEE/CVF conference on computer vision and pattern recognition*, 2023, pp. 9686–9696.
- [11] Y. Du, Z. Zhao, Y. Song, Y. Zhao, F. Su, T. Gong, H. Meng, Strongsort: Make deepsort great again, *IEEE Transactions on Multimedia* (2023).
- [12] Z. Wang, L. Zheng, Y. Liu, S. Wang, Towards real-time multi-object tracking, *The European Conference on Computer Vision (ECCV)* (2020).
- [13] X. Zhou, V. Koltun, P. Krähenbühl, Tracking objects as points, in: *European conference on computer vision*, Springer, 2020, pp. 474–490.

- [14] Y. Zhang, C. Wang, X. Wang, W. Zeng, W. Liu, Fairmot: On the fairness of detection and re-identification in multiple object tracking, *International journal of computer vision* 129 (2021) 3069–3087.
- [15] E. Yu, Z. Li, S. Han, H. Wang, Relationtrack: Relation-aware multiple object tracking with decoupled representation, *IEEE Transactions on Multimedia* (2022).
- [16] S. Hao, P. Liu, Y. Zhan, K. Jin, Z. Liu, M. Song, J.-N. Hwang, G. Wang, Divotrack: A novel dataset and baseline method for cross-view multi-object tracking in diverse open scenes, *International Journal of Computer Vision* 132 (4) (2024) 1075–1090.
- [17] S. Chen, E. Yu, J. Li, W. Tao, Delving into the trajectory long-tail distribution for multi-object tracking, in: *Proceedings of the IEEE/CVF Conference on Computer Vision and Pattern Recognition*, 2024, pp. 19341–19351.
- [18] P. Sun, J. Cao, Y. Jiang, R. Zhang, E. Xie, Z. Yuan, C. Wang, P. Luo, Transtrack: Multiple object tracking with transformer, *arXiv preprint arXiv:2012.15460* (2020).
- [19] T. Meinhardt, A. Kirillov, L. Leal-Taixe, C. Feichtenhofer, Trackformer: Multi-object tracking with transformers, in: *Proceedings of the IEEE/CVF conference on computer vision and pattern recognition*, 2022, pp. 8844–8854.
- [20] E. Yu, Z. Li, S. Han, Towards discriminative representation: Multi-view trajectory contrastive learning for online multi-object tracking, in: *Proceedings of the IEEE/CVF Conference on Computer Vision and Pattern Recognition*, 2022, pp. 8834–8843.
- [21] F. Zeng, B. Dong, Y. Zhang, T. Wang, X. Zhang, Y. Wei, Motr: End-to-end multiple-object tracking with transformer, in: *European Conference on Computer Vision*, Springer, 2022, pp. 659–675.
- [22] E. Yu, T. Wang, Z. Li, Y. Zhang, X. Zhang, W. Tao, Motrv3: Release-fetch supervision for end-to-end multi-object tracking, *arXiv preprint arXiv:2305.14298* (2023).
- [23] S. Li, L. Ke, M. Danelljan, L. Piccinelli, M. Segu, L. Van Gool, F. Yu, Matching anything by segmenting anything, in: *Proceedings of the IEEE/CVF Conference on Computer Vision and Pattern Recognition*, 2024, pp. 18963–18973.
- [24] J. Li, E. Yu, S. Chen, W. Tao, Ovtr: End-to-end open-vocabulary multiple object tracking with transformer, *arXiv preprint arXiv:2503.10616* (2025).
- [25] R. Gao, J. Qi, L. Wang, Multiple object tracking as id prediction, in: *Proceedings of the Computer Vision and Pattern Recognition Conference*, 2025, pp. 27883–27893.
- [26] Y. Zhang, D. Wu, W. Han, X. Dong, Bootstrapping referring multi-object tracking, *arXiv preprint arXiv:2406.05039* (2024).
- [27] W. Li, B. Li, J. Wang, W. Meng, J. Zhang, X. Zhang, Romot: Referring-expression-comprehension open-set multi-object tracking, *The Visual Computer* 41 (4) (2025) 2425–2437.
- [28] Y. Du, C. Lei, Z. Zhao, F. Su, ikun: Speak to trackers without retraining, in: *Proceedings of the IEEE/CVF Conference on Computer Vision and Pattern Recognition*, 2024, pp. 19135–19144.
- [29] T. Chamiti, L. Di Bella, A. Munteanu, N. Deligiannis, Refergpt: Towards zero-shot referring multi-object tracking, *arXiv preprint arXiv:2504.09195* (2025).
- [30] S. Liang, R. Guan, W. Lian, D. Liu, X. Sun, D. Wu, Y. Yue, W. Ding, H. Xiong, Cognitive disentanglement for referring multi-object tracking, *Information Fusion* (2025) 103349.
- [31] S. Chen, E. Yu, W. Tao, Cross-view referring multi-object tracking, in: *Proceedings of the AAAI Conference on Artificial Intelligence*, Vol. 39, 2025, pp. 2204–2211.
- [32] S. Chen, L. Ma, Y. Yu, E. Yu, L. Liu, W. Tao, Drmot: A dataset and framework for rgb-d referring multi-object tracking, *arXiv preprint arXiv:2602.04692* (2026).
- [33] Y. Yu, Z. Jin, S. Chen, T. Chu, E. Yu, L. Liu, W. Tao, Rt-rmot: A dataset and framework for rgb-thermal referring multi-object tracking, *arXiv preprint arXiv:2602.22033* (2026).
- [34] M. Coketek, H. Ozsoy, N. Imamoglu, C. Ozcinar, I. Ayhan, E. Erdem, A. Erdem, Spherical vision transformers for audio-visual saliency prediction in 360° videos, *IEEE transactions on pattern analysis and machine intelligence* (2025).

- [35] J. Deng, Y. Wang, H. Meng, Z. Hou, Y. Chang, G. Chen, Omnistere: Real-time omnidirectional depth estimation with multiview fisheye cameras, in: Proceedings of the Computer Vision and Pattern Recognition Conference, 2025, pp. 1003–1012.
- [36] Y. Zhou, T. Zhang, D. Zhang, S. Ji, X. Li, L. Qi, Dense360: Dense understanding from omnidirectional panoramas, arXiv preprint arXiv:2506.14471 (2025).
- [37] W. Zhang, D. Xiao, A. Dai, Y. Liu, T. Pan, S. Wen, L. Chen, L. Wang, Leader360v: The large-scale, real-world 360 video dataset for multi-task learning in diverse environment, arXiv preprint arXiv:2506.14271 (2025).
- [38] K. Xie, A. Sabour, J. Huang, D. Paschalidou, G. Klar, U. Iqbal, S. Fidler, X. Zeng, Videopanda: Video panoramic diffusion with multi-view attention, arXiv preprint arXiv:2504.11389 (2025).
- [39] Z. Yang, W. Ge, Y. Li, J. Chen, H. Li, M. An, F. Kang, H. Xue, B. Xu, Y. Yin, et al., Matrix-3d: Omnidirectional explorable 3d world generation, arXiv preprint arXiv:2508.08086 (2025).
- [40] Y. Xia, S. Weng, S. Yang, J. Liu, C. Zhu, M. Teng, Z. Jia, H. Jiang, B. Shi, Panowan: Lifting diffusion video generation models to 360  $\{\deg\}$  with latitude/longitude-aware mechanisms, arXiv preprint arXiv:2505.22016 (2025).
- [41] Y. He, W. Yu, J. Han, X. Wei, X. Hong, Y. Gong, Know your surroundings: Panoramic multi-object tracking by multimodality collaboration, in: Proceedings of the IEEE/CVF Conference on Computer Vision and Pattern Recognition, 2021, pp. 2969–2980.
- [42] K. Luo, H. Shi, S. Wu, F. Teng, M. Duan, C. Huang, Y. Wang, K. Wang, K. Yang, Omnidirectional multi-object tracking, in: Proceedings of the Computer Vision and Pattern Recognition Conference, 2025, pp. 21959–21969.
- [43] A. Radford, J. W. Kim, C. Hallacy, A. Ramesh, G. Goh, S. Agarwal, G. Sastry, A. Askell, P. Mishkin, J. Clark, et al., Learning transferable visual models from natural language supervision, in: International conference on machine learning, PMLR, 2021, pp. 8748–8763.
- [44] J. Achiam, S. Adler, S. Agarwal, L. Ahmad, I. Akkaya, F. L. Aleman, D. Almeida, J. Al-tenschmidt, S. Altman, S. Anadkat, et al., Gpt-4 technical report, arXiv preprint arXiv:2303.08774 (2023).
- [45] G. Team, R. Anil, S. Borgeaud, J.-B. Alayrac, J. Yu, R. Soricut, J. Schalkwyk, A. M. Dai, A. Hauth, K. Millican, et al., Gemini: a family of highly capable multimodal models, arXiv preprint arXiv:2312.11805 (2023).
- [46] K. Zheng, X. He, X. E. Wang, Minigpt-5: Interleaved vision-and-language generation via generative vokens, arXiv preprint arXiv:2310.02239 (2023).
- [47] O. Team, Internvl2: Better than the best—expanding performance boundaries of open-source multimodal models with the progressive scaling strategy (2024).
- [48] X. Shen, Y. Xiong, C. Zhao, L. Wu, J. Chen, C. Zhu, Z. Liu, F. Xiao, B. Varadarajan, F. Bordes, et al., Longvu: Spatiotemporal adaptive compression for long video-language understanding, arXiv preprint arXiv:2410.17434 (2024).
- [49] H. Zhang, Y. Wang, Y. Tang, Y. Liu, J. Feng, J. Dai, X. Jin, Flash-vstream: Memory-based real-time understanding for long video streams, arXiv preprint arXiv:2406.08085 (2024).
- [50] B. Xiao, H. Wu, W. Xu, X. Dai, H. Hu, Y. Lu, M. Zeng, C. Liu, L. Yuan, Florence-2: Advancing a unified representation for a variety of vision tasks, in: Proceedings of the IEEE/CVF Conference on Computer Vision and Pattern Recognition, 2024, pp. 4818–4829.
- [51] X. Wang, X. Zhang, Z. Luo, Q. Sun, Y. Cui, J. Wang, F. Zhang, Y. Wang, Z. Li, Q. Yu, et al., Emu3: Next-token prediction is all you need, arXiv preprint arXiv:2409.18869 (2024).
- [52] P. Agrawal, S. Antoniak, E. B. Hanna, B. Bout, D. Chaplot, J. Chudnovsky, D. Costa, B. De Monicault, S. Garg, T. Gervet, et al., Pixtral 12b, arXiv preprint arXiv:2410.07073 (2024).
- [53] Y. Sun, F. Yu, S. Chen, Y. Zhang, J. Huang, Y. Li, C. Li, C. Wang, Chattracker: Enhancing visual tracking performance via chatting with multimodal large language model, Advances in Neural Information Processing Systems 37 (2024) 39303–39324.

- [54] W. Wang, Z. Gao, L. Gu, H. Pu, L. Cui, X. Wei, Z. Liu, L. Jing, S. Ye, J. Shao, et al., Internvl3.5: Advancing open-source multimodal models in versatility, reasoning, and efficiency, arXiv preprint arXiv:2508.18265 (2025).
- [55] H. Lu, W. Liu, B. Zhang, B. Wang, K. Dong, B. Liu, J. Sun, T. Ren, Z. Li, H. Yang, et al., Deepseek-vl: towards real-world vision-language understanding, arXiv preprint arXiv:2403.05525 (2024).
- [56] H. Liu, C. Li, Y. Li, B. Li, Y. Zhang, S. Shen, Y. J. Lee, Lllavanext: Improved reasoning, ocr, and world knowledge (2024).